Bioorg. Med. Chem. Lett. 48 (2021) 128266

Contents lists available at ScienceDirect

Bioorganic & Medicinal Chemistry Letters

journal homepage: www.elsevier.com/locate/bmcl

2-(Halogenated Phenyl) acetamides and propanamides as potent TRPV1 antagonists

Jin Mi Kang [a], Sun Ok Kwon [a], Jihyae Ann [a], Sunho Lee [a], Changhoon Kim [a], Nayeon Do [a], Jin Ju Jeong [a], Peter M. Blumberg [a], Heejin Ha [b], Thi Ngoc Lan Vu [c], Sanghee Yoon [c], Sun Choi [c], Robert Frank-Foltyn [d], Bernhard Lesch [d], Gregor Bahrenberg [d], Hannelore Stockhausen [d], Thomas Christoph [d], Jeewoo Lee [a,*]

[a] Laboratory of Medicinal Chemistry, College of Pharmacy, Seoul National University, Seoul 08826, Republic of Korea
[b] Medifron DBT, Seoul 08502, Republic of Korea
[c] Global AI Drug Discovery Center, College of Pharmacy and Graduate School of Pharmaceutical Sciences, Ewha Womans University, Seoul 03760, Republic of Korea
[d] Grünenthal Innovation, Grünenthal GmbH, D-52078 Aachen, Germany

ARTICLE INFO

Keywords:
Vanilloid Receptor 1
TRPV1 Antagonist
Analgesic

ABSTRACT

A series consisting of 117 2-(halogenated phenyl) acetamide and propanamide analogs were investigated as TRPV1 antagonists. The structure–activity analysis targeting their three pharmacophoric regions indicated that halogenated phenyl A-region analogs exhibited a broad functional profile ranging from agonism to antagonism. Among the compounds, antagonists **28** and **92** exhibited potent antagonism toward capsaicin for *h*TRPV1 with $K_{i\,[CAP]}$ = 2.6 and 6.9 nM, respectively. Further, antagonist **92** displayed promising analgesic activity *in vivo* in both phases of the formalin mouse pain model. A molecular modeling study of **92** indicated that the two fluoro groups in the A-region made hydrophobic interactions with the receptor.

The transient receptor potential vanilloid 1 (TRPV1) is a molecular integrator of nociceptive stimuli expressed in primary sensory neurons.[1–6] Functionally, it is a nonselective cation channel and is activated by vanilloids such as capsaicin and resiniferatoxin and by noxious stimuli including heat, low pH or inflammatory mediators.[7–10] Blockade of TRPV1 activation is considered a promising therapeutic target for the treatment of neuropathic pain.

However, despite of the extensive efforts made for the development of clinical TRPV1 antagonists as novel non-opioid analgesics,[11] almost all of the antagonists to date have failed in the clinical stage mostly due to mechanism-associated side effects such as hyperthermia or loss of sensitivity to thermal pain. The current understanding is that the side effects are linked to antagonists that block all activation modes of TRPV1, and in particular that hyperthermia is associated with the inhibition of the proton activation mode of TRPV1 channel.[12,13] Since the different modes of TRPV1 activation are differentially associated with the pattern of response at the whole animal level, antagonists with selectivity among the activation modes of TRPV1 would be of particular interest for avoidance of such side effects.

In support of this concept, it was recently reported that a mode-selective TRPV1 antagonist that potently blocked channel activation by capsaicin, but did not block activation by protons, did not cause hyperthermia.[13] The goal of the present study is to further explore structure–activity relationships for TRPV1 antagonists. The longer term objective will be to integrate these insights to identify activator-selective TRPV1 antagonists to yield novel analgesics with reduced side effects as second-generation antagonists.[14,15]

Previously, we have investigated a series of 2-(3-fluoro-4-methylsulfonamidophenyl)propanamides as *h*TRPV1 antagonists. Among them, compounds **1**–**3** displayed exceptionally potent antagonism to capsaicin ($K_{i[CAP]}$ = 0.2 nM for **1**, $K_{i[CAP]}$ = 0.1 nM for **2** and **3**) and blocked the hypothermic effect of capsaicin *in vivo*, consistent with their *in vitro* mechanism (Fig. 1).[16,17] Their activity was stereospecific for the *S*-configuration. Whereas antagonists **1** and **2** showed full antagonism to all activators, antagonist **3** exhibited antagonism selective for capsaicin and *N*-arachidonoyl dopamine (NADA) but not for low pH or heat (45 °C). The pharmacophoric region of the antagonistic scaffold can be divided into so-called A- (red), B- (black) and C-regions (blue), previously designated for capsaicin (Fig. 1).

The basis for the high potencies of the antagonists was revealed by

* Corresponding author.
E-mail address: jeewoo@snu.ac.kr (J. Lee).

https://doi.org/10.1016/j.bmcl.2021.128266
Received 14 June 2021; Received in revised form 1 July 2021; Accepted 11 July 2021
Available online 14 July 2021

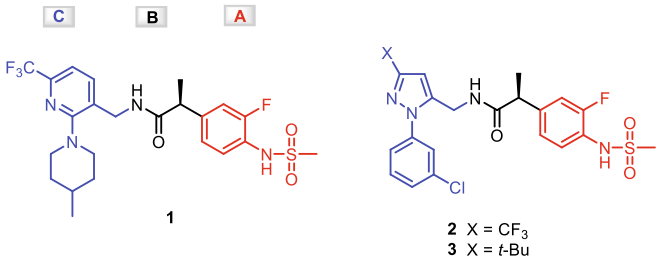

Fig. 1. Prototype TRPV1 antagonists.

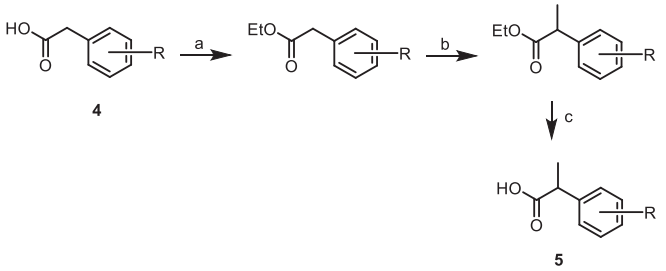

Scheme 1. Synthesis of the halogenated phenyl A-region *Reagents and conditions*: (a) EtOH, H_2SO_4, reflux, 2 h; (b) MeI, NaH, DMF, 0 °C, 2 h; (c) LiOH, r.t., THF-H_2O (1:1), overnight.

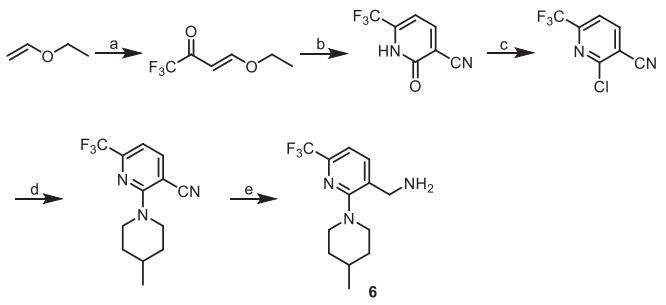

Scheme 2. Synthesis of the 6-trifluoromethylpyridine C-region. *Reagents and conditions*: (a) $(CF_3CO_2)_2O$, pyridine; (b) $NCCH_2CONH_2$, K_2CO_3, toluene; (c) $POCl_3$; (d) 4-methylpiperidine; (e) BH_3-SMe_2 in THF.

molecular docking studies using our established *h*TRPV1 homology model, demonstrating that the two hydrophobic interactions in the C-region were critical for potent antagonism. For instance, the 2-substituent and the 6-CF_3 group in the pyridine for **1** and the 1-substituent and the 3-CF_3/*t*-butyl in pyrazole for **2** and **3** made hydrophobic interactions with pockets composed of Met514/Leu515 and Leu547/Thr550 regions, respectively, or vice versa. Therefore, the pyridine and pyrazole C-region of 1–3 have been employed as prototype C-region for the respective optimization of the A- and B-regions.[16,17] For the discovery of a clinical candidate for neuropathic pain, we have extensively modified the three pharmacophoric regions of our template. Much of our effort has been directed at the structure activity relationship (SAR) of the C-region[18] and the A-region[19–21].

Here, as part of our continuing efforts to optimize the A-region of our TRPV1 antagonistic template, we have investigated 2-(halogenated phenyl) acetamides and propanamides fixed with the prototype C-regions of **1**–**3**. In this study, we describe the syntheses of a series of halogenated phenyl A-region derivatives and characterize their antagonism toward activation of *h*TRPV1 by capsaicin. With a selected potent antagonist in the series, we further characterize its analgesic effect in a pain model and performed a molecular modeling study to elucidate the key binding interactions.

Commercially available 2-(halogenated phenyl) acetic acids as an A-region were employed for the synthesis of the final compounds. For the synthesis of 2-(halogenated phenyl) propionic acid as an A-region (Scheme 1), the corresponding acetic acids (**4**) were converted to ethyl esters, which were α-alkylated with methyl iodide and then hydrolyzed under basic conditions to provide propionic acids (**5**), respectively.

For the synthesis of (2-(4-methylpiperidin-1-yl)-6-(trifluoromethyl) pyridin-3-yl)methanamine (**6**) as a C-region (Scheme 2), trifluoromethylacetylation of ethylvinyl ether followed by condensation with cyanoacetamide provided the pyridone intermediate, which was readily converted to 2-chloropyridine by $POCl_3$ and then its nitrile group was reduced to yield the 6-trifluoromethylpyridine C-region amine.

For the synthesis of (1-(3-chlorophenyl)-3-trifluoromethyl-1*H*-pyrazol-5-yl)methylamine (**7**) as a C-region (Scheme 3), ethyl trifluoroacetate as a starting material was reduced to the corresponding aldehyde and then was condensed with 3-chlorophenyl hydrazine to afford the phenyl hydrazone. The chlorination of hydrazone followed by the reaction with 2-chloroacrylonitrile provided 4-cyanopyrazole which was reduced to afford the 3-trifluoromethylpyrazole C-region amine (**7**).

For the synthesis of (1-(3-chlorophenyl)-3-*t*-butyl-1*H*-pyrazol-5-yl) methylamine (**8**) as a C-region (Scheme 4), 4,4-Dimethyl-3-oxopentanenitrile was condensed with 3-chlorophenyl hydrazine to provide 1-(3-chlorophenyl) 3-*t*-butyl-5-aminopyrazole whose amine was converted to the corresponding nitrile group and then reduced to afford the 3-*t*-butylpyrazole C-region amine (**8**).

The prepared 2-(halogenated phenyl) acetic (**4**) and propionic (**5**) acids (A-region) were coupled with 6-trifluoromethylpyridine (**6**), 3-

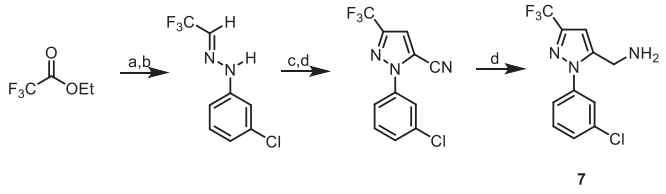

Scheme 3. Synthesis of the 3-trifluoromethylpyrazole C-region. Reagents and conditions: (a) $LiAlH_4$, Et_2O, −78 °C, 2 h; (b) (3-Cl)Ph-$NHNH_2$, EtOH, reflux, 5 h; (c) NCS, DMF, r.t.; (d) 2-chloroacrylonitrile, TEA, toluene, 80 °C, 20 h; (e) $LiAlH_4$, THF, 0 °C to r.t., 3 h.

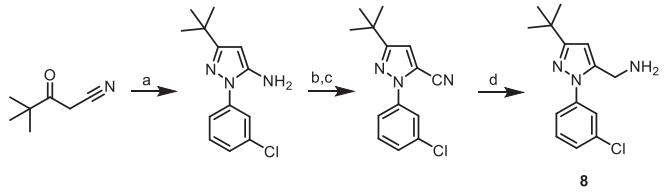

Scheme 4. Synthesis of the 3-*t*-butylpyrazole C-region. Reagents and conditions: (a) (3-Cl)Ph-$NHNH_2$, EtOH:H_2O (1:1), reflux, overnight; (b) *t*-BuONO, CuI, CH_3CN, 0 °C to 65 °C; (c) $Zn(CN)_2$, $Pd(PPh_3)_4$, DMF, reflux, overnight; (d) $LiAlH_4$, THF, 0 °C to r.t., 1 h.

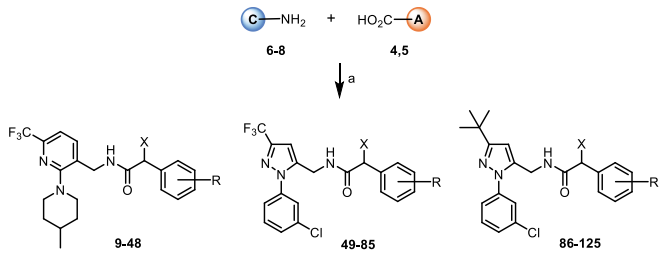

Scheme 5. Synthesis of final amide compounds. *Reagents and conditions*: (a) 1-(3-dimethylaminopropyl)-3-ethyl-carbodiimide hydrochloride, 1-hydroxybenzotriazole, DMF, r.t., overnight.

Table 1
*In vitro h*TRPV1 functional activities for 2-(halogenated phenyl) acetamides and propanamides with a 6-trifluoromethylpyridine C-region.

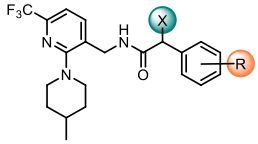

	X	R	$K_{i[CAP]}$ (nM)[a]
1 (rac)	CH_3	3-F, 4-NHMs	0.3
9	H	2-F	9.9
10	H	3-F	34
11	H	4-F	AG
12	H	2-Cl	9.1
13	H	3-Cl	6.1
14	H	4-Cl	AG
15	H	2,3-F_2	9.4
16	H	2,4-F_2	AG
17	H	2,5-F_2	30
18	H	2,6-F_2	38
19	H	3,4-F_2	pAG
20	H	3,5-F_2	10.3
21	H	2,3-Cl_2	4.9
22	H	2,4-Cl_2	46
23	H	2,6-Cl_2	39.7
24	H	3,4-Cl_2	6.7
25	H	3-F, 4-Cl	pAG
26	H	3-Cl, 4-F	12.9
27	H	3-CF_3, 4-F	9.8
28	H	2-F, 6-Cl	2.6
29	H	2-Cl, 4-F	14.2
30	CH_3	2-F	60.4
31	CH_3	3-F	AG
32	CH_3	4-F	AG
33	CH_3	2-Cl	72.8
34	CH_3	3-Cl	13.8
35	CH_3	4-Cl	pAG
36	CH_3	2,3-F_2	31.4
37	CH_3	2,4-F_2	pAG
38	CH_3	2,5-F_2	59.6
39	CH_3	2,6-F_2	110
40	CH_3	3,4-F_2	AG
41	CH_3	3,5-F_2	24.7
42	CH_3	2,3-Cl_2	75.3
43	CH_3	2,4-Cl_2	NE
44	CH_3	3,4-Cl_2	pAG
45	CH_3	3-F, 4-Cl	pAG
46	CH_3	3-Cl, 4-F	17.7
47	CH_3	3-CF_3, 4-F	10.8
48	CH_3	2-Cl, 4-F	AG

[a] Values from triplicate experiments (AG: agonist, pAG: partial agonist, NE: not effective).

Table 2
*In vitro h*TRPV1 functional activities for 2-(halogenated phenyl) acetamides and propanamides with a 3-trifluoromethylpyrazole C-region.

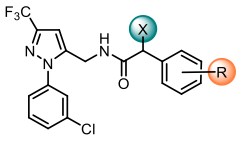

	X	R	$K_{i[CAP]}$ (nM)[a]
2 (rac)	CH_3	3-F, 4-NHMs	0.3
49	H	2-F	80.7
50	H	3-F	51.8
51	H	4-F	pAG
52	H	2-Cl	26.2
53	H	3-Cl	6.2
54	H	4-Cl	6.3
55	H	2,3-F_2	11.5
56	H	2,4-F_2	43.3
57	H	2,5-F_2	58.9
58	H	2,6-F_2	WE
59	H	3,4-F_2	pAG
60	H	3,5-F_2	13.7
61	H	2,3-Cl_2	22.6
62	H	2,4-Cl_2	NE
63	H	2,6-Cl_2	WE
64	H	3,4-Cl_2	3.8
65	H	3-F, 4-Cl	20.9
66	H	3-Cl, 4-F	26.9
67	H	3-CF_3, 4-F	11.9
68	H	2-F, 6-Cl	35.7
69	H	2-Cl, 4-F	38.8
70	CH_3	2-F	NT
71	CH_3	3-F	pAG
72	CH_3	4-F	pAG
73	CH_3	2-Cl	41.9
74	CH_3	3-Cl	pAG
75	CH_3	4-Cl	pAG
76	CH_3	2,3-F_2	18.4
77	CH_3	2,4-F_2	pAG
78	CH_3	2,5-F_2	56.7
79	CH_3	2,6-F_2	33.6
80	CH_3	3,4-F_2	pAG
81	CH_3	3,5-F_2	pAG
82	CH_3	2,3-Cl_2	13.2
83	CH_3	2,4-Cl_2	NE
84	CH_3	3,4-Cl_2	7.6
85	CH_3	3-F, 4-Cl	9.5

[a] Values from triplicate experiments (AG: agonist, pAG: partial agonist, NE: not effective).

trifluoromethylpyrazole (**7**) or 3-*t*-butylpyrazole (**8**) amines (C-region) to provide the final amide compounds (**9**–**125**), respectively, whose structures were confirmed by spectroscopic analysis (Scheme 5).[22]

The *in vitro* assay for TRPV1 antagonism was performed using a fluorometric imaging plate reader (FLIPR) with *h*TRPV1 heterologously expressed in Chinese hamster ovary (CHO) cells.[16] The activity of the synthesized compounds was measured by inhibition of TRPV1 activation by capsaicin (100 nM) and expressed as the inhibition constant ($K_{i[CAP]}$). The results are summarized in Tables 1–3.

For the SAR study of the halogenated phenyl A-region, monofluorophenyl, monochlorophenyl, difluorophenyl, dichlorophenyl, and mixed dihalophenyl analogs were examined.

First, we investigated the functional activities of the 2-(halogenated phenyl) acetamides (**9**–**29**) and propanamides (**30**–**48**) with the 6-trifluoromethylpyridine C-region (Table 1).

In the analogs of monohalophenyl acetamide, the 2-fluoro isomer (**9**) showed potent antagonism, but the 3-fluoro (**10**) and 4-fluoro (**11**) isomers exhibited moderate antagonism and agonism, respectively. In the other hand, whereas the 2-chloro and 3-chloro isomers exhibited potent antagonism, the 4-chloro isomer was an agonist like the 4-fluoro isomer. In the analogs of dihalophenyl acetamide, most isomers exhibited antagonism, but some showed different functional profiles. The 2,4-difluoro isomer (**16**) displayed agonism, and the 3,4-difluoro (**19**) and the 3-fluoro-4-chloro isomers (**25**) showed partial agonism. Among the antagonists, 2-fluoro-6-chloro isomer (**28**) displayed the most potent antagonism with $K_{i[CAP]} = 2.6$ nM. In the analogs of monohalophenyl propanamide, most compounds showed less potent antagonism compared to the corresponding acetamide surrogate. Among them, the 3-fluoro and 4-fluoro isomers were agonists. In the analogs of dihalophenyl propanamide, the compounds showed a similar pattern to that of monohalophenyl propanamide. Among them, the 3,4-difluoro isomer and the 2-chloro-4-fluoro isomer were found to be agonists.

In conclusion, the SAR analysis of pyridine C-region analogs indicated that (1) acetamide B-region analogs were more potent than the corresponding propanamide B-region surrogates. (2) The order of antagonism in positional isomers of the acetamide analogs was 2-isomer > 3-isomer > 4-isomer and the 4-halo substituent shifted functional activity to agonism for both acetamide and propanamide.

Table 3
In vitro *h*TRPV1 functional activities for 2-(halogenated phenyl) acetamides and propanamides with a 3-*t*-butylpyrazole C-region.

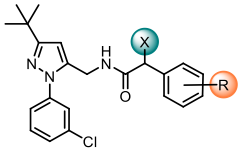

	X	R	$K_{i[CAP]}$ (nM)[a]
3 (rac)	CH_3	3-F, 4-NHMs	0.3
86	H	2-F	pAG
87	H	3-F	AG
88	H	4-F	AG
89	H	2-Cl	7.7
90	H	3-Cl	AG
91	H	4-Cl	AG
92	H	2,3-F_2	6.9
93	H	2,4-F_2	pAG
94	H	2,5-F_2	pAG
95	H	2,6-F_2	49.6
96	H	3,4-F_2	AG
97	H	3,5-F_2	pAG
98	H	2,3-Cl_2	4.0
99	H	2,4-Cl_2	16.7
100	H	2,6-Cl_2	NE
101	H	3,4-Cl_2	pAG
102	H	3-F, 4-Cl	pAG
103	H	3-Cl, 4-F	AG
104	H	3-CF_3, 4-F	8.8
105	H	2-F, 6-Cl	19
106	H	2-Cl, 4-F	19.9
107	CH_3	2-F	AG
108	CH_3	3-F	AG
109	CH_3	4-F	AG
110	CH_3	2-Cl	pAG
111	CH_3	3-Cl	AG
112	CH_3	4-Cl	AG
113	CH_3	2,3-F_2	pAG
114	CH_3	2,4-F_2	AG
115	CH_3	2,5-F_2	pAG
116	CH_3	2,6-F_2	pAG
117	CH_3	3,4-F_2	AG
118	CH_3	3,5-F_2	AG
119	CH_3	2,3-Cl_2	pAG
120	CH_3	2,4-Cl_2	AG
121	CH_3	3,4-Cl_2	AG
122	CH_3	3-F, 4-Cl	AG
123	CH_3	3-Cl, 4-F	AG
124	CH_3	3-CF_3, 4-F	59
125	CH_3	2-Cl, 4-F	26

[a] Values from triplicate experiments (AG: agonist, pAG: partial agonist, NE: not effective).

Secondly, we investigated the functional activities of the 2-(halogenated phenyl) acetamides (**49**–**69**) and propanamide (**70**–**85**) with a 3-trifluoromethylpyrazole C-region (Table 2).

In the analogs of monohalophenyl acetamide, the chloro isomers showed higher antagonism than the corresponding fluoro isomers. Among the compounds, the 3-chloro and 4-chloro isomers displayed potent antagonism. In the analogs of dihalophenyl acetamide, most compounds exhibited moderate to weak antagonism except for the 3,4-dichloro isomer, probably due to their high lipophilicity. In the analogs of monohalophenyl and dihalophenyl propanamide, similar to the SAR for the pyridine C-region, propanamide analogs were found to be less potent than the corresponding acetamide surrogates, showing weak antagonism or partial agonism.

The SAR analysis of 3-trifluoromethylpyrazole C-region analogs indicated that (1) acetamide B-region analogs were more potent than the corresponding propanamide B-region surrogates. (2) In positional isomers of the acetamide analogs, the 3-chloro and 4-chloro isomers showed potent antagonism and the additive 3,4-dichloro isomer provided high potency.

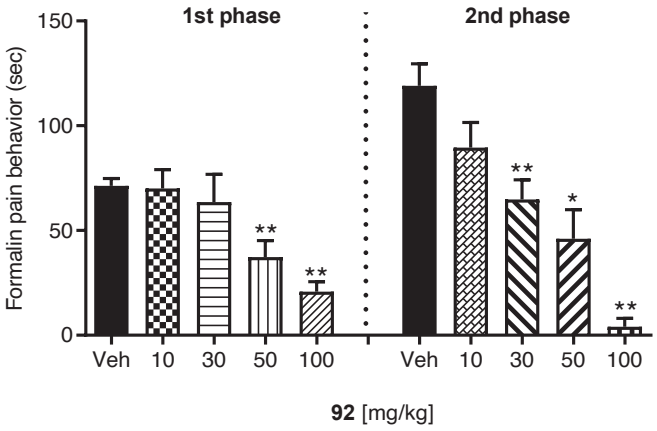

Fig. 2. Analgesic activity of **92** in the formalin pain model by i.p. injection.

Thirdly, we investigated the functional activities of the 2-(halogenated phenyl) acetamides (**86**–**106**) and propanamides (**107**–**125**) with a 3-*t*-butylpyrazole C-region (Table 3).

In the series of TRPV1 ligands, the 3-*t*-butylpyrazole C-region generally shifted the functional activity to agonism compared to the pyridine and 3-trifluoromethyl pyrazole C-regions as examined previously[17]. In the analogs of monohalophenyl acetamide, most compounds were agonists or partial agonists except for the 2-chloro isomer. In the analogs of dihalophenyl acetamide, the compounds also showed partial agonism or agonism due to the C-region. In the analogs of monohalophenyl and dihalophenyl propanamide, most compounds proved to be agonists or partial agonists.

The SAR analysis of 3-*t*-butylpyrazole C-region analogs indicated that (1) similar to the SAR for the other C-regions, acetamide B-region analogs were more potent than the corresponding propanamide B-region surrogates. (2) The C-region shifted the activity to agonism, rendering most compounds partial agonists or agonists.

Lipophilicity of TRPV1 ligands is one of important factors determining the agonism/antagonism potency because the binding site for the ligand is located by the inner surface of the cell membrane. As the lipophilicity of the ligand increases, its potency is usually enhanced. However, excessive lipophilicity causes low solubility, which will affect bioavailability. In fact, a number of clinical antagonists have suffered from this solubility issue. Since dichlorophenyl analogs have very high lipophilicity (ex. **64**: cLogP = 5.85), they are thus less appealing candidates for further study in terms of drug development.

To evaluate the *in vivo* activity of selected potent antagonists, two antagonists **28** ($K_{i[CAP]}$ = 2.6 nM) and **92** ($K_{i[CAP]}$ = 6.9 nM) were examined for their antinociceptive activity after administration by intraperitoneal injection (i.p.) in the formalin mouse model.[23]

Whereas compound **28** exhibited weak analgesic activity, compound **92** demonstrated reasonable analgesic activity in both the 1st and 2nd phase in a dose-dependent manner, providing an ED_{50} of 50.5 mg/kg in the 1st phase and 29.5 mg/kg in the 2nd phase, respectively (Fig. 2). The weak *in vivo* activity of **28** was not further explored, but could reflect, among other explanations, either a problem of bioavailability due to its high lipophilicity or a species difference between mouse and human TRPV1. In additiom, to examine the effect of antagonist **92** on thermoregulation, the body temperature was measured after i.p. administration of 10 mg/kg of the compound in mice. It did not cause any hyperthermia at given dose.

Binding modes of compound **92** were investigated with our recently published homology models of *h*TRPV1,[21] which were constructed based on the cryo-EM structure of *r*TRPV1 complexed with the antagonist, capsazepine. In order to consider the flexibility of *h*TRPV1, we

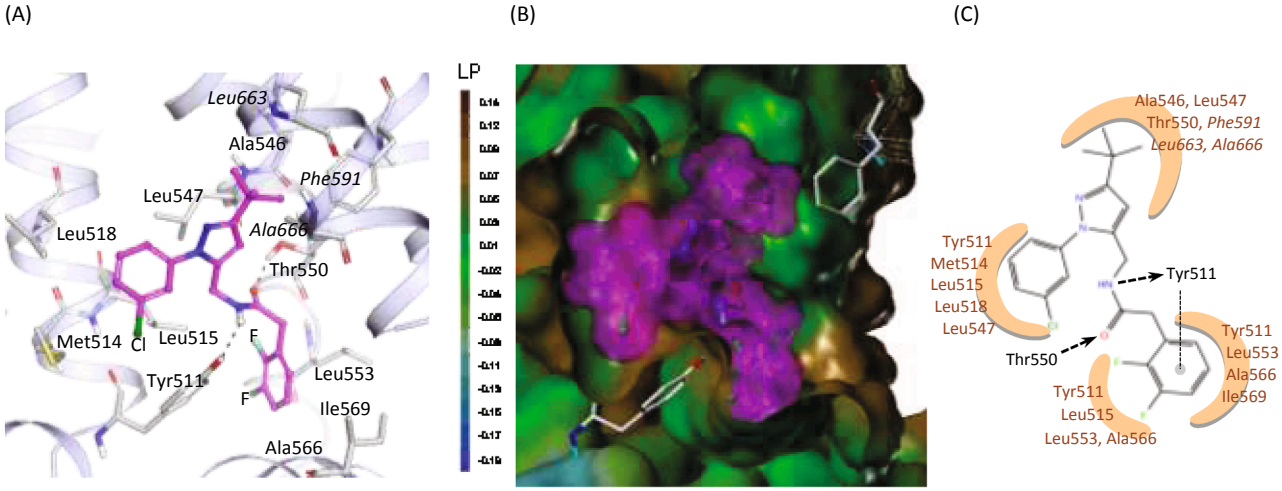

Fig. 3. Binding mode of **92** in the *h*TRPV1 homology model. (A) Binding mode of 92 represented in ball-and-sticks with the atoms colored as: C in magenta, F in green–blue, N in blue, O in red, Cl in green, H in white. The interacting residues are depicted in sticks with their carbon atoms in grey. The secondary structure of the *h*TRPV1 model is displayed in ribbon. This representation is generated with PyMOL Molecular Graphics System version 1.8.6.2 (Schrodinger, LLC, NY, USA). (B) The Fast Connolly surface presented with the lipophilic potential property of *h*TRPV1 and the van der Waals surface of 92, created by MOLCAD program implemented in SYBYL-X 2.1.1 (Tripos Int., St. Louis, MO, USA). For clarity, the surface of *h*TRPV1 is Z-clipped and that of the ligand is colored by magenta. (C) 2-D representation of the binding interactions between 92 and *h*TRPV1. Hydrophobic interactions are displayed with bronze curved patches. Hydrogen bonds are marked in black-dashed lines, and nonpolar hydrogen atoms are undisplayed for clarity.

applied the ensemble docking and induced fit docking using the six discrete conformations of the homology models derived from the clustering after the molecular dynamics simulations.[24]

As shown in Fig. 3, the A-region of **92** occupies the bottom of the vanilloid pocket with the phenyl ring making hydrophobic interactions with Tyr511, Leu553, Ala566 and Ile569, along with the π–π stacking with Tyr511. Moreover, both of the two fluoro groups in the phenyl ring form hydrophobic interactions: the 2-fluoro group with Tyr511, Leu515 and Leu553; and the 3-fluoro group with Tyr511, Leu553 and Ala566.

The amide group in the B-region participates in two hydrogen bonds with Tyr511 and Thr550, which were observed in other amide-containing TRPV1 ligands in previous studies.[17,21,25] These interactions allow the C-region of the ligand to hold the position where the *t*-butyl-pyrazole group occupies the shallow upper niche, resulting in hydrophobic interactions with Ala546, Leu547, Thr550, Phe591, Leu663, and Ala666. In addition, the chlorophenyl group settles down in the middle open region and makes hydrophobic interactions with Tyr511, Met514, Leu515, Leu518 and Leu547.

In summary, a series of 2-(halogenated phenyl) acetamides and propanamides were investigated as *h*TRPV1 antagonists. The SAR study was conducted systematically in a mono(di)halo-substituted phenyl A-region fixed with three prototype C-regions previously studied to optimize the antagonism to capsaicin.

The analysis of SAR based on pharmacophoric region indicated that (1) in the SAR of the A-region, the positional potency depends on the C-region, but a 2,3-difluorophenyl A-region always provided potent antagonism regardless of the B- and C-regions. (2) In the SAR of the B-region, the acetamide B-region is more potent than the corresponding propanamide B-region surrogate. (3) In the C-region SAR, the order of antagonistic tendency is as follows: 3-trifluoromethylpyrazole > 6-trifluoromethylpyridine > 3-*t*-butylpyrazole. In particular, most compounds with a 1-(3-chlorophenyl)-3-*t*-butylpyrazole C-region displayed agonism or partial agonism.

Further *in vivo* studies with the selected potent antagonists indicated that compound **92** showed promising analgesic activity in formalin mouse model.

The molecular modeling study of **92** indicated that the two fluoro groups in the A-region made hydrophobic interactions, while the B- and C-regions made the similar interactions with the receptor as previously examined.

Declaration of Competing Interest

The authors declare that they have no known competing financial interests or personal relationships that could have appeared to influence the work reported in this paper.

Acknowledgments

This work was supported by the Midcareer Researcher Program (NRF-2019R1A2C2006837 and NRF-2020R1A2C2101636) funded by the National Research Foundation of Korea (NRF).

References

1 Szallasi A, Blumberg PM. Vanilloid (capsaicin) receptor and mechanisms. *Pharmacol Rev*. 1999;51:159–211.
2 Moran MM, McAlexander MA, Bíró T, Szallasi A. Transient receptor potential channels as therapeutic targets. *Nat Rev Drug Dis*. 2011;10:601–620.
3 Aghazadeh Tabrizi M, Baraldi PG, Baraldi S, Gessi S, Merighi S, Borea PA. Medicinal chemistry, pharmacology, and clinical implications of TRPV1 receptor antagonists. *Med Res Rev*. 2017;37:936–983.
4 Basso L, Altier C. Transient receptor potential channels in neuropathic pain. *Curr Opin Pharmacol*. 2017;32:9–15.
5 Iftinca M, Defaye M, Altier C. TRPV1-targeted drugs in development for human pain conditions. *Drugs*. 2021;81:7–27.
6 Gladkikh IN, Sintsova OV, Leychenko EV, Kozlov SA. TRPV1 ion channel: structure features, activity modulators, and therapeutic potential. *Biochemistry (Moscow)*. 2021;86:S50–S70.
7 Caterina MJ, Schumacher MA, Tominaga M, Rosen TA, Levine JD, Julius D. The capsaicin receptor: a heat-activated ion channel in the pain pathway. *Nature*. 1997;389:816–824.
8 Tominaga M, Caterina MJ, Malmberg AB, et al. The cloned capsaicin receptor integrates multiple pain-producing stimuli. *Neuron*. 1998;21:531–543.
9 Morales-Lazaro SL, Simon SA, Rosenbaum T. The role of endogenous molecules in modulating pain through transient receptor potential vanilloid 1 (TRPV1). *J Physiol*. 2013;591:3109–3121.
10 Szolcsányi J, Sándor Z. Multisteric TRPV1 nocisensor: a target for analgesic. *Trend Pharmacol Sci*. 2012;33:646–655.
11 (a) Kym PR, Kort ME, Hutchins CW. Analgesic potential of TRPV1 antagonists. *Biochem Pharmacol*. 2009;78:211.(b) Wong GY, Gavva NR. Therapeutic potential of vanilloid receptor TRPV1 agonists and antagonists as analgesics: recent advances and setbacks. *Brain Res Rev*. 2009;60:267–277.(c) Gunthorpe MJ, Chizh BA. Clinical development of TRPV1 antagonists: targeting a pivotal point in the pain pathway. *Drug Discovery Today*. 2009;14:56–67.(d) Lazar J, Gharat L, Khairathkar-Joshi N, Blumberg PM, Szallasi A. Screening TRPV1 antagonists for the treatment of pain:

lessons learned over a decade. *Expert Opin Drug Dis.* 2009;4:159–180.(e) Voight EA, Kort ME. Transient receptor potential vanilloid-1 antagonists: a survey of recent patent literature. *Expert Opin Ther Pat.* 2010;20:1–16.(f) Szallasi A, Sheta M. Targeting TRPV1 for pain relief: limits, losers and laurels. *Expert Opin Invest Drug.* 2012;21:1351–1369.(g) De Petrocellis L, Moriello AS. Modulation of the TRPV1 channel: current clinical trials and recent patents with focus on neurological conditions. *Recent Pat on CNS Drug Dis.* 2013;8:180–204.(h) Lee Y, Hong S, Cui M, Sharma PK, Lee J, Choi S. Transient receptor potential vanilloid type 1 antagonists: a patent review (2011–2014). *Expert Opin Ther Pat.* 2015;25:291–318.

12 Garami A, Shimansky YP, Pakai E, Oliveira DL, Gavva NR, Romanovsky AA. Contributions of different modes of TRPV1 activation to TRPV1 antagonist-induced hyperthermia. *J Neurosci.* 2010;30:1435–1440.

13 Reilly RM, McDonald HA, Puttfarcken PS, et al. Pharmacology of modality-specific transient receptor potential vanilloid-1 antagonists that do not alter body temperature. *J Pharm Exp Ther.* 2012;342:416–428.

14 Garami A, Pakai E, McDonald HA, et al. TRPV1 antagonists that cause hypothermia, instead of hyperthermia, in rodents: Compound's pharmacological profiles, in vivo targets, thermoeffectors recruited and implications for drug development. *Acta Physiol.* 2018;223, e13038.

15 Garami A, Shimansky YP, Rumbus Z, et al. Hyperthermia induced by transient receptor potential vanilloid-1 (TRPV1) antagonists in human clinical trials: Insights from mathematical modeling and meta-analysis. *Pharmacol Therapeut.* 2020;208, 107474.

16 Kim MS, Ryu H, Kang DW, et al., 2-(3-Fluoro-4-methylsulfonylaminophenyl) propanamides as potent transient receptor potential vanilloid 1 (TRPV1) antagonists: Structure-activity relationships of 2-amino derivatives in the N-(6-trifluoromethylpyridin-3-ylmethyl) C-Region. J Med Chem. 2012;55:8392-8408.

17 Lee S, Kim C, Ann J, et al. Pyrazole C-region analogues of 2-(3-fluoro-4-methylsulfonylaminophenyl)propanamides as potent TRPV1 antagonists. *Bioorg Med Chem Lett.* 2017;27:4383–4388.

18 Ahn S, Kim YS, Kim MS, et al., Discovery of indane propanamides as potent and selective TRPV1 antagonists. Bioorg Med Chem Lett. 2020;30:126838. ref 10-21.

19 Kim C, Ann J, Lee S, et al. 4-Aminophenyl acetamides and propanamides as potent transient receptor potential vanilloid 1 (TRPV1) ligands. *Bioorg Med Chem.* 2018;26: 4509–4517.

20 Kang JM, Kwon SO, Ann J, et al. Discovery of 1-(1H-indazol-4-yl)-3-((1-phenyl-1H-pyrazol-5-yl)methyl) ureas as potent and thermoneutral TRPV1 antagonists. *Bioorg Med Chem Lett.* 2020;30, 127548.

21 Thorat SA, Lee Y, Jung A, et al. Discovery of benzopyridone-based transient receptor potential vanilloid 1 agonists and antagonists and the structural elucidation of their activity shift. *J Med Chem.* 2021;64:370–384.

22 Spectra for representative compound 92: 64 % yield, ivory powder, mp = 108-110 °C; 1H-NMR (400 MHz, DMSO) δ 8.62 (t, J = 5.3 Hz, 1H), 7.53 (d, J = 2.3 Hz, 1H), 7.40 - 7.48 (m, 3H), 7.23 - 7.30 (m, 1H), 7.04 - 7.12 (m, 2H), 6.25 (s, 1H), 4.33 - 4.37 (d, J = 5.6 Hz, 2H), 3.51 (s, 2H), 1.22 (s, 9H); HRMS (FAB) calcd for C22H22ClF2N3O [M + H]+ 417.1419, found 418.1480.

23 Tjølsen A, Berge OG, Hunskaar S, Rosland JH, Hole K. The formalin test: an evaluation of the method. *Pain.* 1992;51:5–17.

24 For the docking studies, our established six representative conformations of the homology models, complexed with CAPZ, were prepared with 'Protein Preparation Wizard' implemented in Maestro v. 11.7 (Schrodinger, LLC, NY, USA), which includes optimizing hydrogen bonds with the protonation state of residues at pH 7.2, and minimizing the protein structures with an optimized potential for liquid simulation (OPLS) 3 force field. The ligand structure was prepared with the 'LigPrep' module, using an OPLS3 force field for structure energy minimization. The ensemble docking was performed using 'Virtual Screening Workflow' protocol with standard precision (SP). For each of the prepared hTRPV1 homology models, the grid boxes were centered at the respective CAPZ molecules with the uniform innerbox size of 10 Å, 14 Å, 19 Å. The scaling of ligand van der Waals radii for nonpolar atoms was set at 0.8, partial charge cutoff value at 0.15, and number of poses to generate at 30. Then, the induced fit docking was performed with 'Induced Fit Docking' module with SP using the ensemble docking results. The grid box was centered at the CAPZ molecule with the inner box lengths of 19 Å. Up to 30 best modes were kept based on IFDScore, keeping the other settings as default. For the analysis of the docking results, LigandScout 4.4 (Inte:Ligand GmbH, Vienna, Austria) was also utilized. All computational studies were undertaken on an Intel® Xeon® Gold 6254 CPU 3.10 GHz workstation with Linux CentOS release 7.6.

25 Cui M, Gosu V, Basith S, Hong S, Choi S. Polymodal transient receptor potential vanilloid type 1 nocisensor: structure, modulators, and therapeutic applications. *Adv Protein Chem Struct Biol.* 2016;104:81–125.